Proceedings of the 16th European VLBI Network Symposium
Ros, E., Benke, P., Dzib, S., Rottmann, I., & Zensus, J.A. (eds.)
September 2nd-6th 2024, Bonn, Germany

The KVN-Mopra VLBI Network: System Performance, Early Results, and Recent Updates

W. Y. Cheong[1,2], S.-S. Lee[1,2], D.-Y. Byun[1,2], H.-W. Jeong[1,2], S. Kim[1,2], and J. Hodgson[3]

[1] University of Science and Technology, 217 Gajeong-ro, Yuseong-gu, Daejeon 34113, Republic of Korea
[2] Korea Astronomy and Space Science Institute, 776 Daedeok-daero, Yuseong-gu, Daejeon 34055, Republic of Korea
[3] Department of Physics and Astronomy, Sejong University, 209 Neungdong-ro, Gwangjin-gu, Seoul, Republic of Korea

Abstract. We have conducted joint VLBI observations between the Korean VLBI Network (KVN) and a radio telescope, Mopra, located in Australia. We have successfully observed at all three common frequency bands of 22, 43, and 86 GHz, including the application of linear-to-circular polarization conversion for Mopra at 43 and 86 GHz. The VLBI (or synthesized) beam minor axis is found to be 0.2, 0.1, 0.05 mas at 22, 43, 86 GHz respectively due to that of the KVN-Mopra baselines, while the major axis is comparable to the KVN-only beam (6, 3, 1.5 mas). Coherence times were found to be approximately 10 seconds at 86 GHz. Nevertheless, the (up to) 16 Gbps observations provided by the OCTAD backend and Mark6 recorder allowed the detection of fringes on the KVN-Mopra baselines for a number of sources at 86 GHz with flux densities down to 0.2-0.3 Jy. With careful calibration and imaging, we are able to produce high-resolution CLEAN images, with residual calibration errors of ∼4% in amplitude and ∼3 degrees in phase at 22 GHz. We also find that direct model fitting to the measured visibilities and closure quantities of the data allows us to reconstruct the sub-mas source structure in the vicinity of the radio cores. Based on our initial success, we have expanded our observations to relative astrometry observations with the East Asian VLBI Network + Mopra, and regular joint observations between the KVN, Mopra, and the Hartebeesthoek 26m radio telescope in South Africa.

1. Introduction

Global VLBI observations with baseline lengths of ∼10,000 km allow detailed imaging at sub-milliarcsecond resolutions at the expense of reduced observation cadence. Given the typical variability of blazars, investigation of flaring AGNs benefits from high-cadence and long-term monitoring of targets of interest. Observations with a VLBI array consisting of a smaller number of antennas allow the high-cadence observations necessary to probe the high angular resolution and high cadence variability characteristics of AGN radio cores (i.e., compact and bright emission regions in radio VLBI images) at the expense of sparse sampling in the *uv*-space. In order to achieve weekly to biweekly observations of AGNs at sub-mas angular resolution, we have started joint observations between the Korean VLBI Network (KVN, Lee et al., 2014) and the Mopra telescope in Australia (Ladd et al., 2005; Urquhart et al., 2010). In this paper, we describe the results from our commissioning and early science observations to evaluate the array sensitivity, imaging capability, and astrometric performance.

2. Observations

We have conducted multiple VLBI observations including the KVN and Mopra. Early commissioning and imaging tests were observed under the experiment code t22sl01. During the epoch of MJD 59725 (t22sl01b), continuum sources 3C 279, 3C 273B, M87, M84, and SGR A* were observed at 22 GHz. Maser sources RT Vir and VX Sgr were included in order to evaluate the relative flux calibration scale between the different stations using the maser template method (e.g., Doeleman et al., 2001; Cho et al., 2017). The observation was recorded in dual polarization, using the OCTAD to observe with 8 subbands of 64 MHz in width. Additionally, a series of fringe detection surveys for a list of 61 continuum sources were conducted during three sessions under the experiment code n22wc02. All three observations were in dual polarization, with each polarization observed in 2 subbands of 512 MHz in width. Finally, we conducted three observations with the East Asian VLBI Network (EAVN) in joint with Mopra under the experiment code a2309. During these observations, we attempted to test fast-switching phase referencing observations at 22 GHz. Observations under the code t22sl01 and n22wc02 were correlated with the KASI DiFX software correlator (Deller et al., 2007). Observations under the code a2309 were correlated with the Korea-Japan Correlation Center (KJCC) hardware correlator (Yeom et al., 2009; Lee et al., 2015). A summary of the VLBI observations used in this paper is given in Table 1.

Table 1. VLBI Observation Overview.

Epoch	Date [UT]	FreqRange [GHz — GHz]	Pol	N_{sub}	BW [MHz]	Sources
t22sl01b	2022-05-26	22.018 — 22.274	Dual	4	64	3C 279, 3C 273B, M87, M84, SGR A*
n22wc02b[a]	2022-09-30	42.468 — 43.492	Dual	2	512	61 individual
n22wc02c[a]	2022-10-28	21.950 — 22.974	Dual	2	512	61 individual
n22wc02d[a]	2022-10-29	85.994 — 87.018	Dual	2	512	61 individual
a2309a[b]	2023-02-23	22.099 — 22.355	LCP	8	32	0215+015, 0216+011, 0235+164, 0239+175, 0556+238, 0601+245
a2309b[b]	2023-04-14	22.099 — 22.355	LCP	8	32	0215+015, 0216+011, 0235+164, 0239+175, 0556+238, 0601+245
a2309c[b]	2023-06-06	22.099 — 22.355	LCP	8	32	0215+015, 0216+011, 0235+164, 0239+175, 0556+238, 0601+245

Note — Summary of the observations used in this paper. The columns are the session code, observation date, frequency range, polarization, number of subbands per polarization, the bandwidth of each subband, and the observed continuum sources.
[a] Amplitude calibration using template T^*_{sys}.
[b] Source list given here is excluding additional calibrators.

3. Results

3.1. The 22, 43, 86 GHz fringe detection surveys

One of the primary points of concern during the early stages of observation was the detectability of sources on the ∼7450 km baseline of the KVN-Mopra, in particular for the higher frequency bands (i.e., 86 GHz). With the absence of both large telescopes and intermediate baselines to Mopra, it was suspected that few sources would be detected on the KVN-to-Mopra baselines. We conducted a fringe detection survey at the three common frequency bands. A preliminary sample of 61 continuum sources, drawn from a pool of science targets and calibrators for future projects, were observed in 1-3 scans per source. It should be noted that this preliminary sample is by no means a complete sample in any form. Due to the absence of simultaneous multifrequency observing capability at Mopra, three consecutive observations were conducted, each at 22, 43, and 86 GHz. The 22 GHz and 86 GHz observations occurred within one day of each other while the 43 GHz observation one month prior.

In contrast to initial concerns, we found that the detection rates were high at both 22 and 43 GHz, with a greater than 80 percent of sources detected on the Mopra baselines. Only ∼60 percent of sources are detected at all at 86 GHz (i.e., on the short KVN-KVN baselines), and approximately half of these detected sources had significant fringes to Mopra as well. We attribute the low detection rates at 86 GHz to be due to the limited baseline sensitivity within the coherence time (∼10 seconds). This may be significantly improved with the installation of quasi-optics at Mopra. Of the sources that were detected, we find that the flux densities on the KVN-Mopra baselines were on average 30-50 percent of those on the KVN-KVN baselines. The distribution of the KVN-Mopra to KVN-KVN baseline correlated flux density ratios is shown in Figure 1.

3.2. K-band imaging with the KVN+Mopra array

The KVN-Mopra baselines are oriented in the North-South direction, limiting the additional sampling in *uv*-space with Earth rotation synthesis. We aimed to study whether we could still construct images with this limited array. A 22 GHz imaging experiment was conducted on 2022 May 26 under the observation code t22sl01b (see Table 1). In addition to the a priori amplitude calibration using system temperature measurements and gain curves, we conducted a second round of amplitude calibration where the relative gains between different stations were calibrated with the autocorrelation spectra of observed masers. Hybrid imaging was conducted in Difmap (Shepherd et al., 1994), during which we alternate between source image reconstruction with the CLEAN algorithm (Högbom, 1974; Schwarz, 1978) and phase-only self-calibration.

Despite the limited *uv*-coverages with the KVN-Mopra array, we find that with careful a priori calibration, we are able to generate high-resolution CLEAN images of compact sources. An example of the calibrated visibilities for 3C 279 is shown in Figure 2, with the KVN-only image and KVN+Mopra image in Figure 3. Due to the *uv*-coverage, the restoring beam of the KVN-Mopra image is elongated with a beam major axis similar to that of the KVN-only data. The beam minor axis of the full KVN-Mopra data is significantly narrower at 0.15 mas, compared to a beam minor axis of 4.43 mas for the KVN-only data. We find that the jet of the source is resolved in the North-South direction. Fitting a simple model of two point sources against the measured closure phases, and comparing against 43 GHz data from the VLBA (Jorstad et al., 2017; Weaver et al., 2022), we find that the KVN-Mopra array can constrain the sub-mas jet of 3C 279 to ΔR.A.$= +56$ μas and ΔDec.$= -200$ μas from the core. Over multiple sources, we obtain CLEAN images with dynamic ranges in the range of 200-1000. The root-mean-square (rms) of the residual maps are 4-16 mJy/beam.

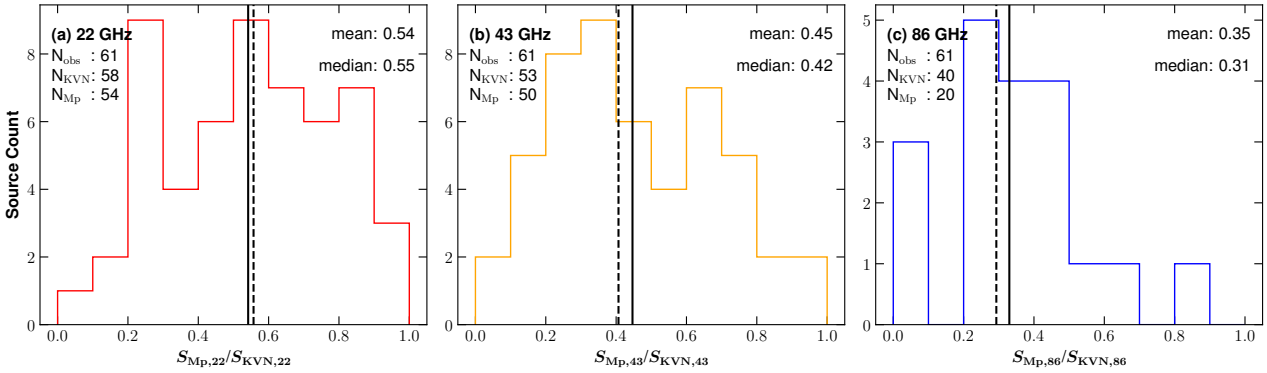

Fig. 1. Correlated flux density ratios between the KVN-Mopra baselines and the KVN-KVN baselines. For each subfigure, $N_{\rm obs}$ is the total number of continuum sources observed, $N_{\rm KVN}$ the number of sources detected on the short KVN-KVN baselines, and $N_{\rm Mp}$ the number of sources detected on the long KVN-Mopra baselines. Vertical solid lines are the mean values of the ratio while the vertial dashed lines are the median.

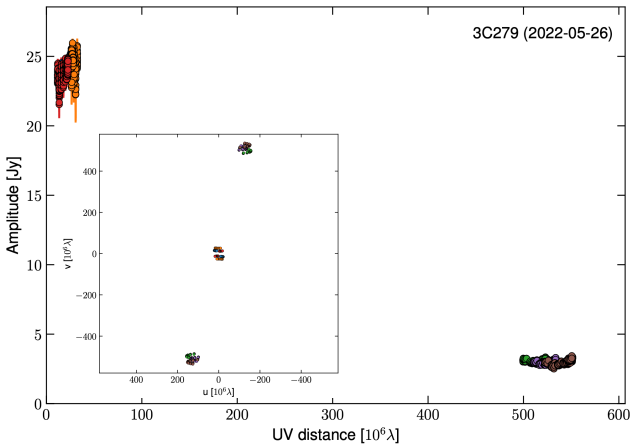

Fig. 2. Correlated flux density of 3C 279 with different uv-distances obtained in the epoch of MJD 59725 (t22sl01b). The subfigure is the uv-coverage of the data. The colors correspond to different baselines.

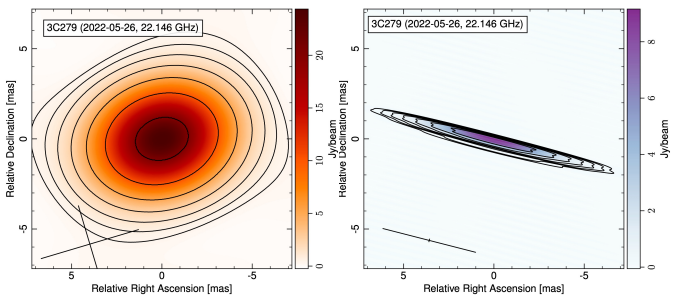

Fig. 3. CLEAN maps of 3C 279 using only the KVN data (left), and the full KVN-Mopra data (right). The restoring beam is plotted in the lower-left of each image.

Residual calibration errors are evaluated to be ∼4% in amplitude and ∼3 degrees in phase at 22 GHz (Cheong et al., in prep).

3.3. EAVN phase referencing observations

We have conducted three EAVN+Mopra experiments to validate the feasibility of performing phase-referencing observations with the joint array. We observed three pairs of sources (0215+015/0216+011, 0235+164/0239+175, 0556+238/0601+245) with angular separations of 0.5-1.4 degrees. A switching cycle of 90 seconds was used, with 35 seconds on the calibrator and 35 seconds on the target, with 10 seconds of slewing time in between. The source 0420-014 was observed as a fringe-finder. We have successfully obtained fringes to all participating stations for all epochs, with all of our calibrator sources (0215+015, 0235+164, 0601+245) detected on the Mopra baselines. A preliminary analysis suggests that phase referencing is possible with Mopra at 22 GHz, with three-epoch source coordinate repeatability rms $\Delta_{\rm rms}$ of 42-180 μas. The exact values for each source may be found in Figure 4. We find that unlike the $\Delta_{\rm rms}$ in right ascension, which is dominated by the astrometric accuracy of the EAVN itself, $\Delta_{\rm rms}$ in declination greatly differs with each source. This strongly hints that there are remaining systematics with associated with the Mopra baselines. These may be further improved with updated station coordinates and calibration of the residual zenith delay of Mopra, as well as a faster switching cycle.

4. Conclusions

We have successfully integrated the Mopra telescope into joint observations with the KVN and EAVN. Fringe detection surveys and imaging observations are ready, while further improvements are required for astrometric observations. We have now transitioned to early science observations. As part of these early science observations, we have initiated a joint monitoring program with the KVN, Mopra, and the Hartebeesthoek 26m radio telescope. These observations allow efficient use of telescope resources, with the same data being used for K-band geodesy and astrophysical studies of AGNs. Since January

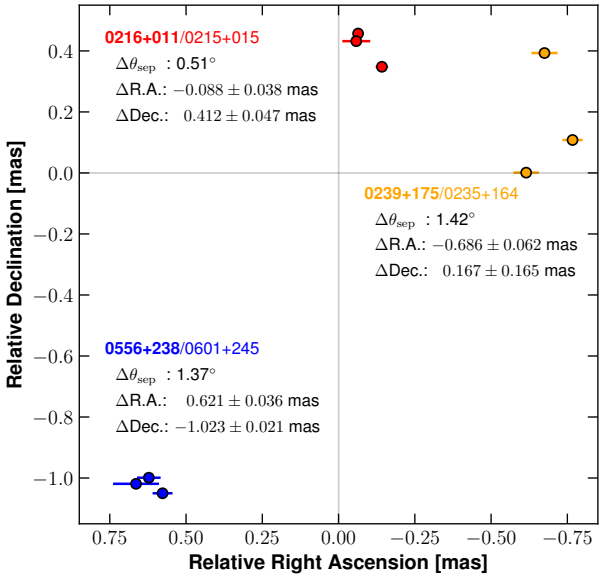

Fig. 4. The mean and rms of the offsets for each pair of sources from our EAVN-Mopra phase referencing observations. Different colors correspond to different source pairs. $\Delta\theta_{\rm sep}$ is the angular separation between the two sources. ΔR.A. and ΔDec. are the mean and rms of the offsets of the phase-referenced target source from the phase center. Error bars correspond to formal thermal uncertainties only.

2023, we have conducted 19 "24-hour sessions" and 14 "5-hour sessions", allowing bi-weekly observations of our core sample at 0.2 mas resolution. Further observations are expected to continue. Description of these observations, as well as there calibration and analysis will be part of a future publication.

Acknowledgements. We are grateful to the staff of the KVN who helped to operate the array and to correlate the data. The KVN and a high-performance computing cluster are facilities operated by the KASI (Korea Astronomy and Space Science Institute). The KVN observations and correlations are supported through the high-speed network connections among the KVN sites provided by the KREONET (Korea Research Environment Open NETwork), which is managed and operated by the KISTI (Korea Institute of Science and Technology Information). The Mopra telescope is part of the Australia Telescope National Facility (https://ror.org/05qajvd42) which is funded by the Australian Government for operation as a National Facility managed by CSIRO. We acknowledge the Gomeroi people as the Traditional Owners of the Observatory site. The University of New South Wales Digital Filter Bank used for the observations with the Mopra Telescope was provided with support from the Australian Research Council. This study makes use of VLBA data from the VLBA-BU Blazar Monitoring Program (BEAM-ME and VLBA-BU-BLAZAR; http://www.bu.edu/blazars/BEAM-ME.html), funded by NASA through the Fermi Guest Investigator Program. The VLBA is an instrument of the National Radio Astronomy Observatory. The National Radio Astronomy Observatory is a facility of the National Science Foundation operated by Associated Universities, Inc.

References

Cho, I., Jung, T., Zhao, G.-Y., et al. 2017, PASJ, 69, 87
Deller, A. T., Tingay, S. J., Bailes, M., et al. 2007, PASP, 119, 318
Doeleman, S. S., Shen, Z.-Q., Rogers, A. E. E., et al. 2001, AJ, 121, 2610
Högbom, J. A. 1974, A&AS, 15, 417
Jorstad, S. G., Marscher, A. P., Morozova, D. A., et al. 2017, ApJ, 846, 98
Ladd, N., Purcell, C., Wong, T., et al. 2005, PASA, 22, 62
Lee, S.-S., Petrov, L., Byun, D.-Y., et al. 2014, AJ, 147, 77
Lee, S.-S., Oh, C. S., Roh, D.-G., et al. 2015, Journal of Korean Astronomical Society, 48, 125
Schwarz, U. J. 1978, A&A, 65, 345
Shepherd, M. C., Pearson, T. J., & Taylor, G. B. 1994, BAAS, 26, 987
Urquhart, J. S., Hoare, M. G., Purcell, C. R., et al. 2010, PASA, 27, 321
Weaver, Z. R., Jorstad, S. G., Marscher, A. P., et al. 2022, ApJS, 260, 12
Yeom, J. H., Oh, S. J., Roh, D. G., et al. 2009, Journal of Astronomy and Space Sciences, 26, 567